

Neutron shielding assessment for the Remote Handling Lower Port rack of ITER

F.Mota¹, N. Casal³, L. Bertalot³, E. Polunovskiy³, F.J.Sanchez¹, J.Sanz², A. Ibarra¹

- 1) Laboratorio Nacional de Fusion, CIEMAT, Madrid, Spain
- 2) Dept. Ingeniería Energética UNED, Madrid, Spain
- 3) ITER Organization, Route de Vinon sur Verdon, Saint Paul Lez Durance, France

Abstract

A neutron shielding assessment of an integrated ITER C-lite neutronics baseline model for the Remote Handling Lower Port rack and port interspace components has been performed. The aim of this paper is to decrease the neutron leakage as a mean to eventually reduce the activation relevant for shutdown dose rates. The performance of the neutron shielding assembled in the baseline model of the Remote Handling Lower Port rack has been assessed. As a mitigation strategy, neutronics calculations have been conducted to evaluate the radiation field during operation in the lower port with the Remote Handling Lower Port rack and the interspace components installed. A progressive improvement of the neutron shielding has been carried out with additional shielding elements including a large shielding block. As a result, the neutron streaming has been significantly reduced along the lower port with a neutron fluence rate in the closure flange in the range of $1 \cdot 10^9$ n/cm²s to $1 \cdot 10^8$ n/cm²s.

DOI10.1016/j.fusengdes.2018.06.023

1. Introduction

The ITER tokamak [1] is equipped with numerous plasma diagnostics to obtain critical information to study and control plasma performance. The diagnostic systems have direct access to the fusion plasma through a series of ports and port plugs included in the design of the vacuum vessel [2]. This work is related to the radiation field during operation and after the shutdown of the Remote Handling Lower Port (RH-LP) and the interspace area (IS). An assessment of the radiation field is essential to address the problem of materials activation and the radiological hazard to personnel during shutdown when the access to the port interspace is scheduled for maintenance. Therefore, an exhaustive radiation field study must be carried out with the aim of minimizing the radiation streaming through ports, diagnostic systems and other penetrations.

The RH-LP Rack is found in three of the lower ports (02, 08 and 14) in the ITER tokamak. The diagnostic equipment foreseen in each rack are the divertor impurity influx monitor (port 02), the divertor Thomson scattering erosion monitor (port 08) and the lower vertical neutron camera (port 14) [3]. In the present work, a generic configuration of the RH-LP rack has been studied, considering a mixture of the different composing materials with the aim to simulate the different filling options, i.e. this paper is a preliminary evaluation of the neutron shielding in order to reduce the large neutron streaming found surrounding the RH-LP rack in the baseline model.

In this paper, neutron transport calculations have been performed to make a shielding assessment of the (RH-LP) area. Different configurations have been proposed in order to reduce the neutron streaming. The objective of the work is to evaluate the radiation field during operation of the lower port with the RH-LP rack and IS components installed. A MCNP model with the most recent components of the RH-LP rack and IS components has been considered for a rigorous analysis

2. Methodology

2.1.- Model Description

SPACECLAIM 2016 [4] software was used to modify and simplify the most recent CAD models of the RH-LP rack and the IS components provided by ITER IO in order to adapt them to be used for neutron transport calculations. The original CAD models, provided by ITER IO, used to obtain the RH-LP MCNP model are described in the ITER IO report [5]. In this report, the simplification process was also described. The simplification of the volumes was made following the criteria described in the neutronics guidelines [6]. The main rules exposed in the neutronics guidelines for the model simplification are the following (here they are quoted literally):

1. Eliminate splines and fillets as required
2. Geometries with simple cells run faster. Split the complex components into simple cells.
3. Respect the gaps parallel to the radiation flux, relevant for streaming
4. Avoid the materials homogenization as much as possible
5. A deviation in material masses greater than 2% is not acceptable, and density correction factors shall be used in the MCNP models. A comparison of the masses of materials in each model for the concerning cells and a table of the densities used in each representation must also be presented. A description of how the corrected densities were derived is also required.
6. Respect the components SS lining or insert them if they should be present but are not.

All these rules have been met except the fourth, as this neutron shielding study has evaluated the neutron shielding of the RH-LP rack baseline model, which is in a preliminary phase of design (materials and geometry). Therefore, once the neutron shielding of the lower port has been improved, a more detailed study will have to be done.

The software used to convert the simplified CAD model into MCNP geometrical model was SuperMC code version 2.3.5, which was developed by the FDS team [7, 8]. The simplified CAD model of the RH-LP rack and the IS components is shown in **Figure 1**.

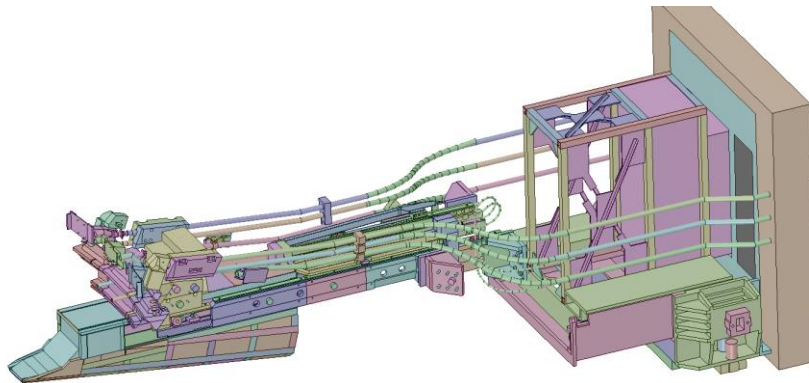


Figure 1.- CAD simplified model of the RH-LP rack and the IS components

The MCNP model of the RH-LP rack and IS components was inserted into the ITER MCNP model C-lite v2 [9, 10]. The ITER MCNP model used was the version DGEPP 01102015 V1.1 04042016 EPY of the C-lite v2 provided by Eduard Polunovskiy in a work communication. This is a modified version of the CLite_v2 model to be able to assemble several components of the lower port, such as the support pads, the central cassette outer rail, the toroidal divertor rails and the pipes supports. The MCNP model of the RH-LP rack and IS components inserted in the C-lite v2 is presented in **Figure 2**.

The Clite_v2 model consists of a 40° regular sector, up to the bioshield, with reflective boundary conditions at lateral sides of the sector. The neutron source specifications correspond to the standard 500 MW of fusion power at steady state with 400 MW of 14.1 MeV D-T neutrons.

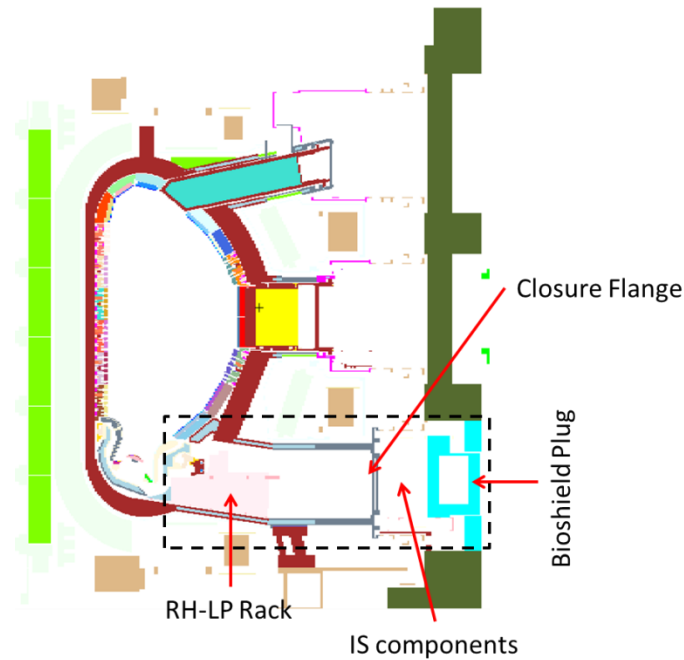


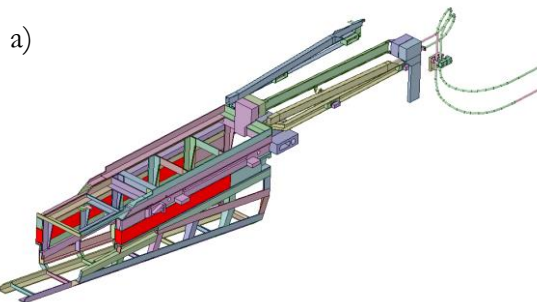
Figure 2.- Vertical cross section of MCNP model C-Lite_v2 with the RH-LP rack and IS components inserted.

2.2.- Material used for the different components.

The materials considered in the RH-LP rack and the IS components comprise the diagnostic components and those associated with the port structure and service elements. The impurity content requirements for the different components were taken from the ITER IO report PIM-169 [11]. The reduction of the content of radiological important impurities, suggested in PIM-169 report, has been implemented to contribute to lower the Shut Down Dose Rate (SDDR) level relevant for the hands-on maintenance of affected systems. In addition, the impurity restrictions were taken into account because this MCNP model was also used for the SDDR calculations shown in ITER IO report_T9B5MM [5].

The restrictions on impurity content, specified in PIM-169 report for diagnostic components, are stronger than the ones assumed for the rest of components. The element content of Co, Ta and Nb in the majority of the steels within the components related to the diagnostic components are 0.03wt.%, 0.01 wt.% and 0.01 wt.%, respectively. While in the rest of components the steel used has a maximum content of 0.05 wt.% of Co. Although for neutron transport calculations the effect of this element restriction is negligible, they have been considered to meet the ITER IO and neutronics guideline [6] requirements and because this neutronics model will be also used for SDDR calculations [5]. These calculations are not shown in this paper for ITER IO confidentiality issues.

The frames of the RH-LP Rack and service arms, shown in Figure 3 a), are made of SS316L(N)-IG with the restriction of chemical elements mentioned above. The structure of the RH-LP rack is a frame in which the shielding blocks are assembled, Figure 3 a). The shielding blocks are composed by a mix of 50%(Vol) SS316LN-IG and 50 % (Vol) boron carbide (B₄C) with a 75% of packaging, i.e. with a density of 3.9185 g/cm³, Figure 3 b). This mixture of materials has been considered to simulate both the shielding blocks and the stainless steel structure to hold them.



b)

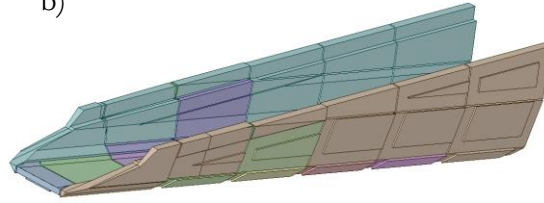


Figure 3.- a) The structure made of SS316L(N)-IG of the RH-LP rack and service arms. The blocks marked in red colour are made of SS316L(N)-IG but with a packaging of 75 % in volume; b) shielding block assembled into the SS316L(N)-IG structure.

The same mix of the stainless steel (SS) and B₄C has been considered for the RH-LP rack inside, with the aim to simulate the diagnostic components and service elements. The density considered for the space useful to hold the diagnostic components and the upper shielding is 3.9185 g/cm³, i.e. 75% of volume is filled, Figure 4. This material configuration has been considered to simulate the inner SS structure holding the diagnostic components, as well as the shielding blocks required to fill up the gaps remaining around the diagnostic components.

However, for the spaces in the upper section of the rack the density considered is 1.306 g/cm³, i.e. with a 25% of packaging volume of the previous mixture of materials mentioned above. It is due to the fact that these volumes will probably hold cooling channels and functional systems, hence, their filling will be lower.

The first part of the rack, shown in blue in Figure 4, named Tip is filled up with a mix of 40%(Vol) B₄C (75% of packaging), 50%(Vol) SS316L(N)-IG and 10%(Vol) water with a density of 4.82 g/cm³. This mixture of materials has been chosen to simulate the SS structure, assembled shielding blocks and the water cooling system of the Tip

Finally, the density considered for the back of the rack interior was adjusted to meet the weight criteria of the ports (they have to weigh less than 10 Tons), being 1.269 g/cm³. In addition, this section of the rack inside will be filled up with ancillary services, then the material packaging will be therefore much lower.

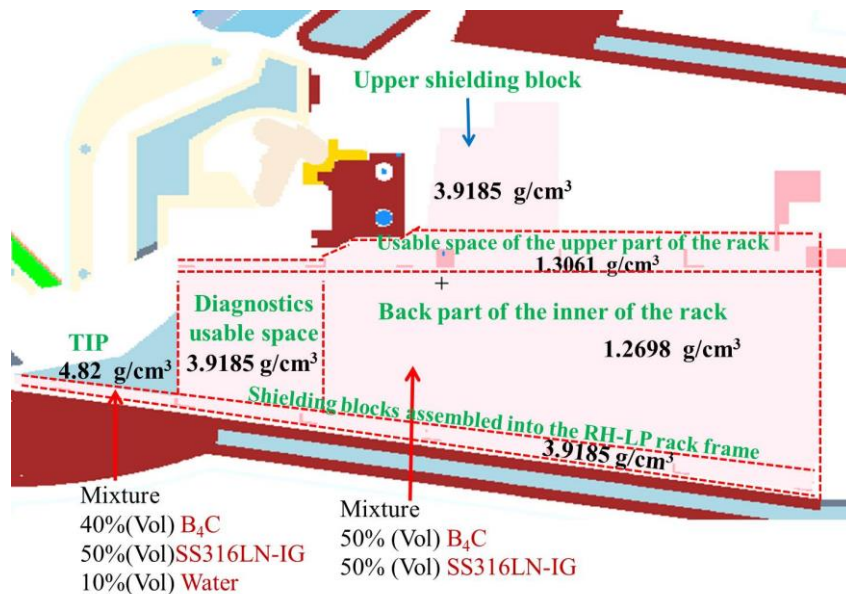


Figure 4.- Longitudinal cross section of the MCNP model showing the material used for the inside of the RH-LP rack. Dotted lines mark the different areas with a different density of the mix of 50% (Vol) B₄C and 50% (Vol) SS316L(N)-IG.

The divertor rails and components, the support pads, the central cassette outer rail, the toroidal divertor rails, the pipes supports and the water cooling pipes made all of SS316L(N)-IG are shown in Figure 5. The SS used for the lower rails, however, was SS316L. They are shown in Figure 6. It is important to insert these components into the model in order to be as realistic as possible in the design, with the aim to identify the gaps whereby the neutrons could escape.

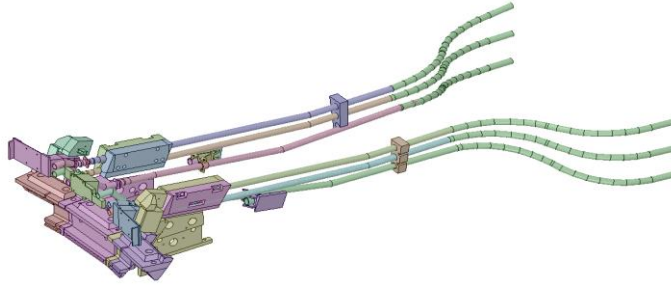


Figure 5.- Components of the Lower Port made of SS316L(N)-IG (maximum 0.05 wt.% of Co)

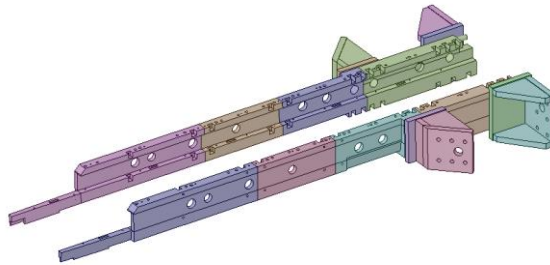


Figure 6.- Components of the lower rails made of SS316L

For IS components the materials used follow the same restrictions about impurity content as in stainless steels for diagnostic elements and non-diagnostic elements presented in the document mentioned above [11].

2.3.- Neutron transport calculation methodology

The neutron transport calculations have been performed using the MCNP5 code version 1.6 [12] and the FENDL 2.1 nuclear data libraries [13]. The neutron source specifications correspond to the standard 500 MW of fusion power at steady state with 400 MW of 14.1 MeV D-T neutrons. In addition, weight window variance reduction techniques have been used to reduce the statistic relative error as much as possible [5]. The weight windows variance reduction map was adjusted with the model density reduction technique to obtain tallies in the whole model. Once an acceptable weight window map is obtained, the original density of the model is recovered for neutron transport calculations.

The 3D mesh-tally used for neutron transport calculations to determine the neutron fluence rates covers the whole volume of the lower port and IS components up to the bioshield plug. The total dimensions considered for each mesh-tally are $1200 \times 360 \times 405 \text{ cm}^3$, and the minimum cubic bin size is $5 \times 5 \times 6 \text{ cm}^3$. Vertical and horizontal sections of the mesh-tally described above are shown in **Figure 7** a) and b) respectively.

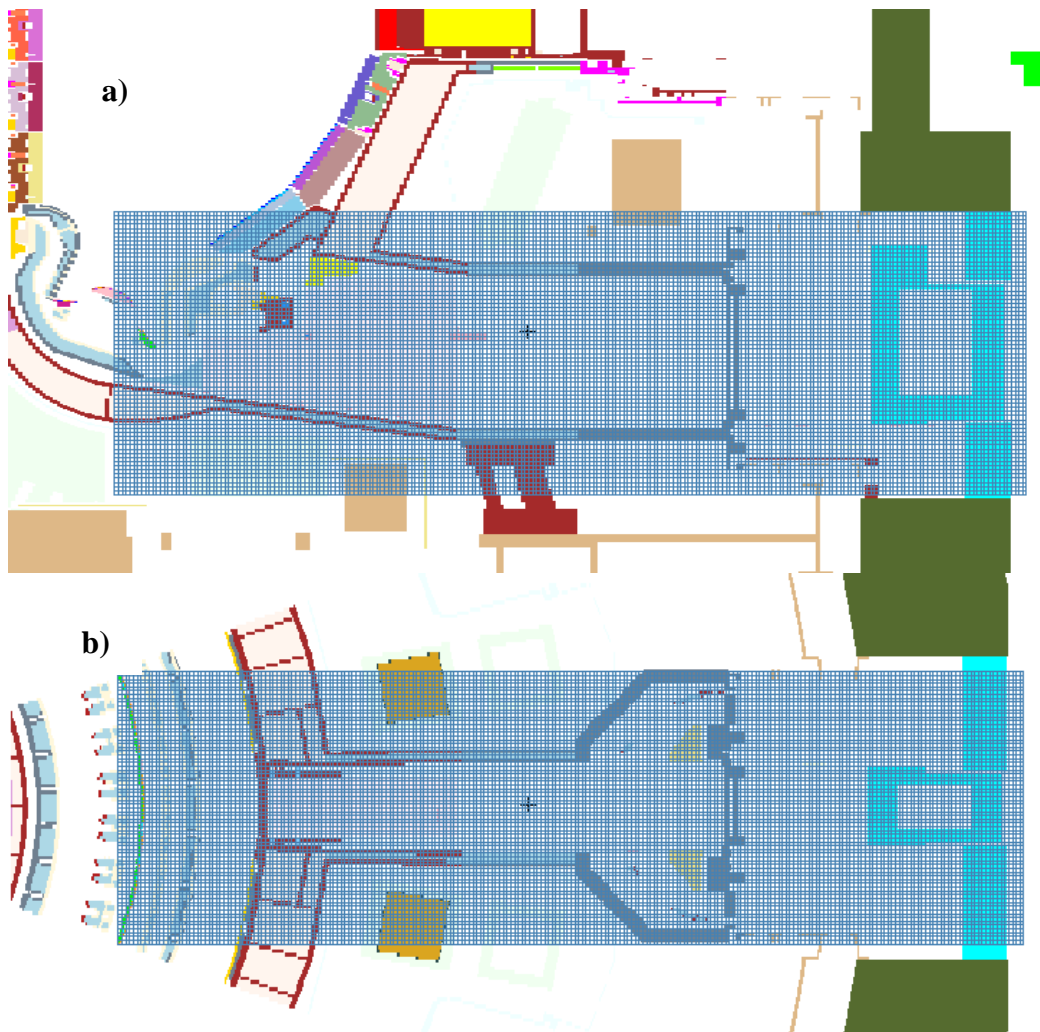


Figure 7.- Mesh-tally used for the neutron fluence rate assessment in the lower port area. a) Vertical and b) horizontal cross sections.

3. Neutron shielding assessment to reduce the neutron streaming

In this section, the neutron fluence rate field is obtained along the lower port area. First, the baseline shielding model was studied and then several shielding blocks have been evaluated in order to reduce the neutron streaming.

3.1.1.- Case 1 (baseline model)

This case consists of the baseline model of the RH-LP and IS components described in the second section, Figure 1. The densities considered for the inner volume of the rack and for the upper shielding blocks have been fitted to meet the limitation of 10 Tons in the total rack weight, Figure 4.

3.1.2.- Case 2 (case 1 + pipe supports + additional upper shielding + belt)

Several elements have been added to Case 1 model to reduce the neutron streaming. The shielding elements added are shown in Figure 8. In order to reduce the lateral neutron streaming it is inserted a new design of pipes supports made of SS316L(N)-IG, Figure 8 1). Besides, an additional shielding block above the upper shielding block has been assembled, closing the gap between the upper shielding block and the top of the lower port, with the aim to decrease the neutron streaming in the upper part of the rack, Figure 8 2). This shielding block is made of B₄C with a density of 2 g/cm³. In the lower part of the rack a belt has been included to reduce the slit between the bottom of the rack and the lower port structure, Figure 8 3). It is also made of SS316L(N)-IG.

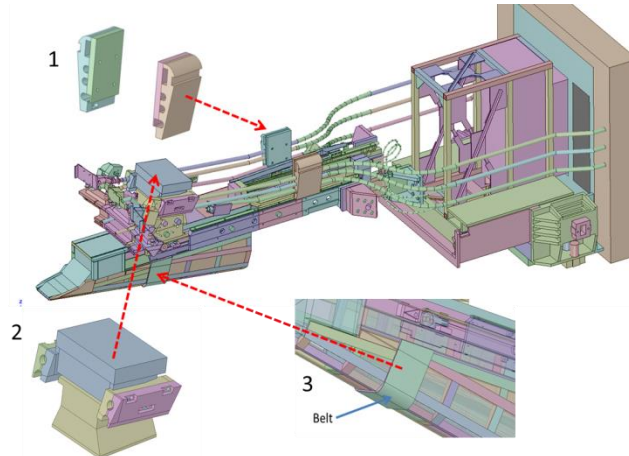


Figure 8.- Case 2 MCNP model; 1) new pipe supports considered; 2) Extended version of the upper shielding; 3) Belt under the rack

3.1.3- Case 3 (case 2 + large additional shielding block behind the upper shielding)

In the case 3 of the shielding assessment, one extension along the rack of the upper shielding block has been tested. Figure 9 shows the 3D model of the case 2 including the upper shielding block extension. In order to insert this model, a minimum distance of 2 cm to the lateral components (pipes and supports) has been considered to meet the distance tolerance criteria. The extended version of the upper shielding block is made of the same mix of B₄C and SS316L(N)-IG considered for the rack inside, (Figure 4), but with the same density used (3.9185 g/cm³) for the baseline upper shielding block. However, the inclusion of this new block in the shielding exceeds the weight limit. With this shielding block the total weight of the RH-LP-rack is 12.4 Tons. Therefore, if this shielding block were approved to be included in the RH-LP rack baseline model, it would be required to revise the 10 Tons weight limitation.

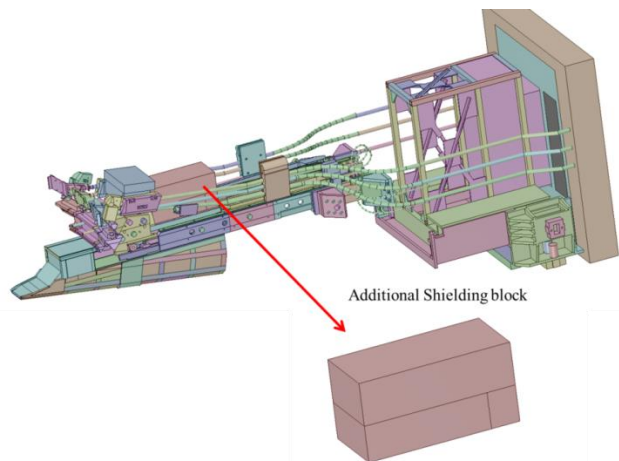


Figure 9.- The MCNP model of the case 3 which is equal to the case 2 but with an additional shielding block at the rear of the rack.

3.2.- Neutron fluence rate calculations

Neutron fluence rates along the lower port area are evaluated considering the three different configurations of the RH-LP rack proposed in the previous subsection. $1 \cdot 10^{11}$ histories have been run in each case assessed with the aim to achieve enough statistics.

Vertical and horizontal cross sections of the 3D neutron fluence rate maps are shown in Figure 10 and Figure 11 respectively for the three cases assessed. The horizontal sections are taken at the height of the upper shielding block ($z=-388$ cm) and the vertical sections correspond to coordinate $y=0$ (refers to a central axis of the model). Comparing the radiation field for the different cases it is easy to realize how

the different shielding blocks considered in the study significantly reduce the neutron streaming along the port.

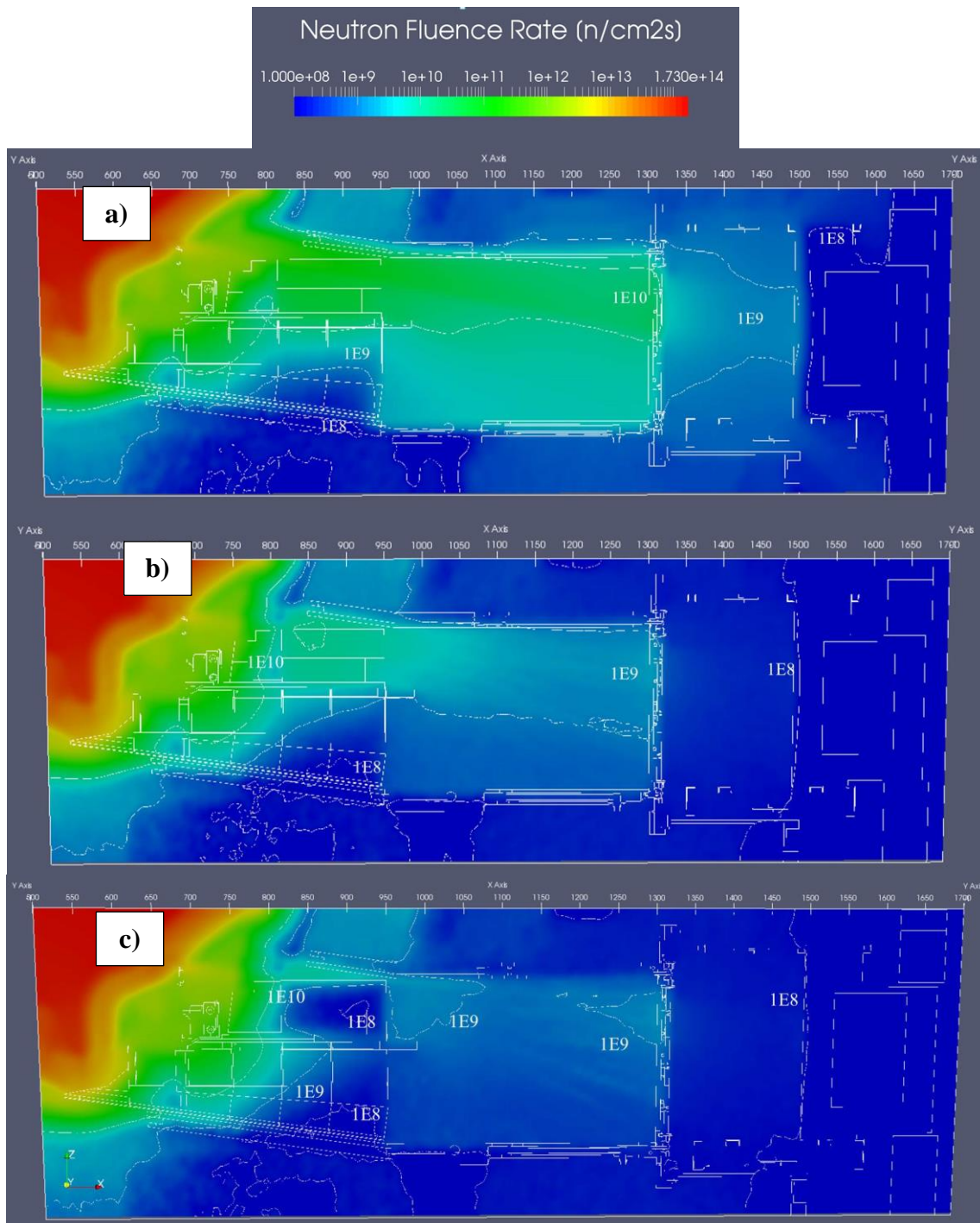


Figure 10.- Vertical section of the neutron fluence rate [n/cm²s] 3D maps; a) Case 1, b) Case 2 and c) Case 3.



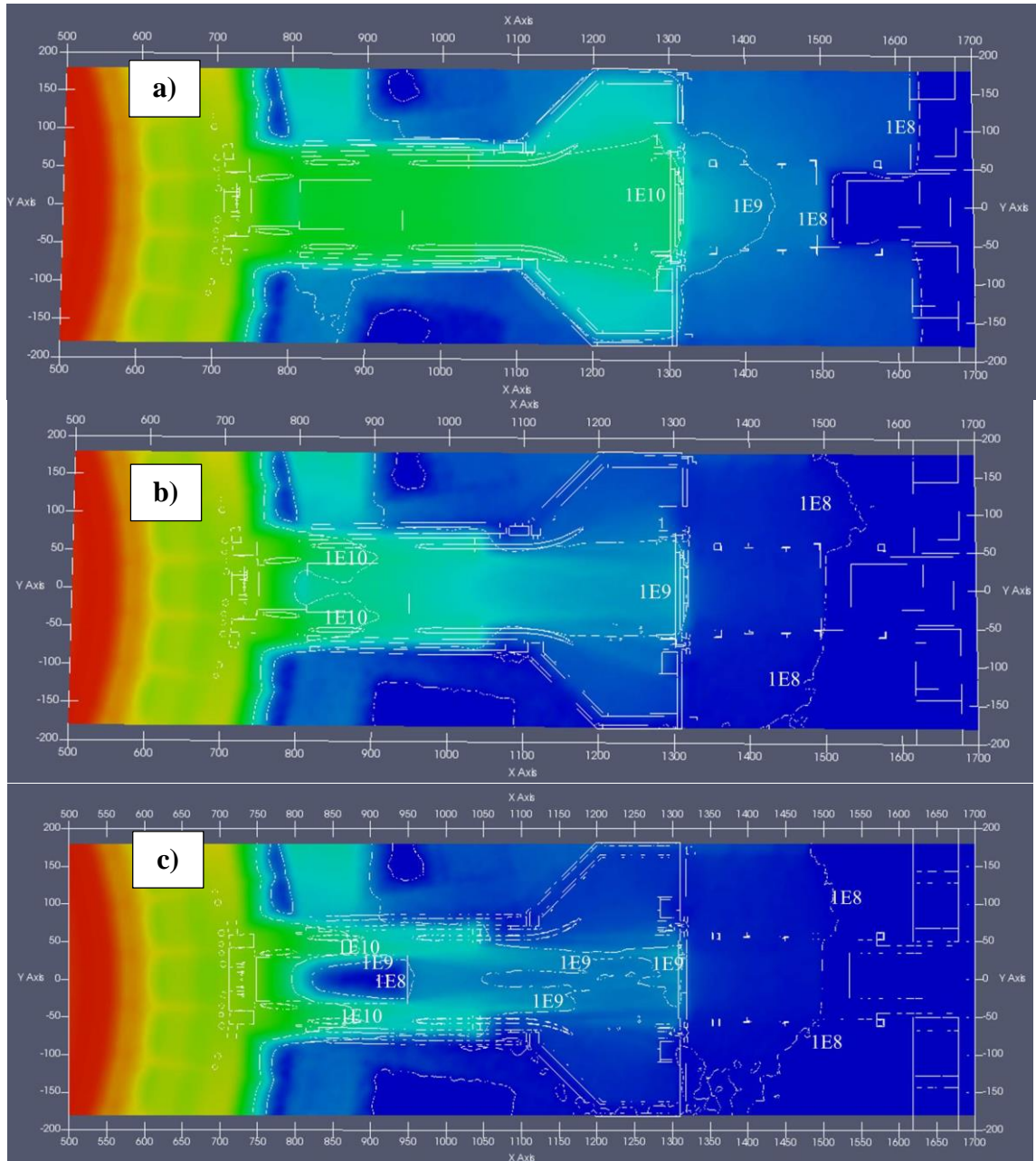


Figure 11.- Horizontal section of the neutron fluence rate [n/cm²s] 3D maps; a) Case 1, b) Case 2 and c) Case 3.

According to the results observed in the figures 10 and 11 the neutron shielding study has been successfully conducted to reduce the neutron streaming, i.e. all tested shielding blocks have worked correctly. They have managed to reduce the neutron fluence rates along the lower port and IS area. With the shielding blocks tested in case 2, the neutron fluence rate in the closure flange decreases one order of magnitude from $1 \cdot 10^{10}$ to $1 \cdot 10^9$ n/cm²s. Moreover, adding to the case 2 the large shielding block behind the upper shielding block described in case 3, the volume with a neutron fluence rate higher than $1 \cdot 10^9$ n/cm²s decreases significantly along the lower port respect to the case 2.

3.3.- Relative error

For quality assurance of the results, it would be desirable that the statistic relative error was less than 0.1 [14] in the area under study, Table 1.

The statistic relative errors obtained for neutron fluence rate are shown in Figure 12 for the three cases evaluated. It is observed that the statistic relative errors are lower than 0.1 in almost all zones studied (in both, the port inner and IS sections), however, this relative error value is exceeded in several

zones around the port. In particular, in case 3, the statistic relative error has increased. This is due to the fact that the lower the neutron streaming the higher the relative error. These relative statistics errors, however, are precise enough for the preliminary shielding assessment described in this work.

Table 1.- Guidelines for interpreting the Relative Error [14]

Range of Relative Error	Quality of the Tally
0.5 to 1	Garbage
0.2 to 0.5	Factor of a few
0.1 to 0.2	Questionable
< 0.10	Generally reliable except for point detector
< 0.05	Generally reliable for point detector

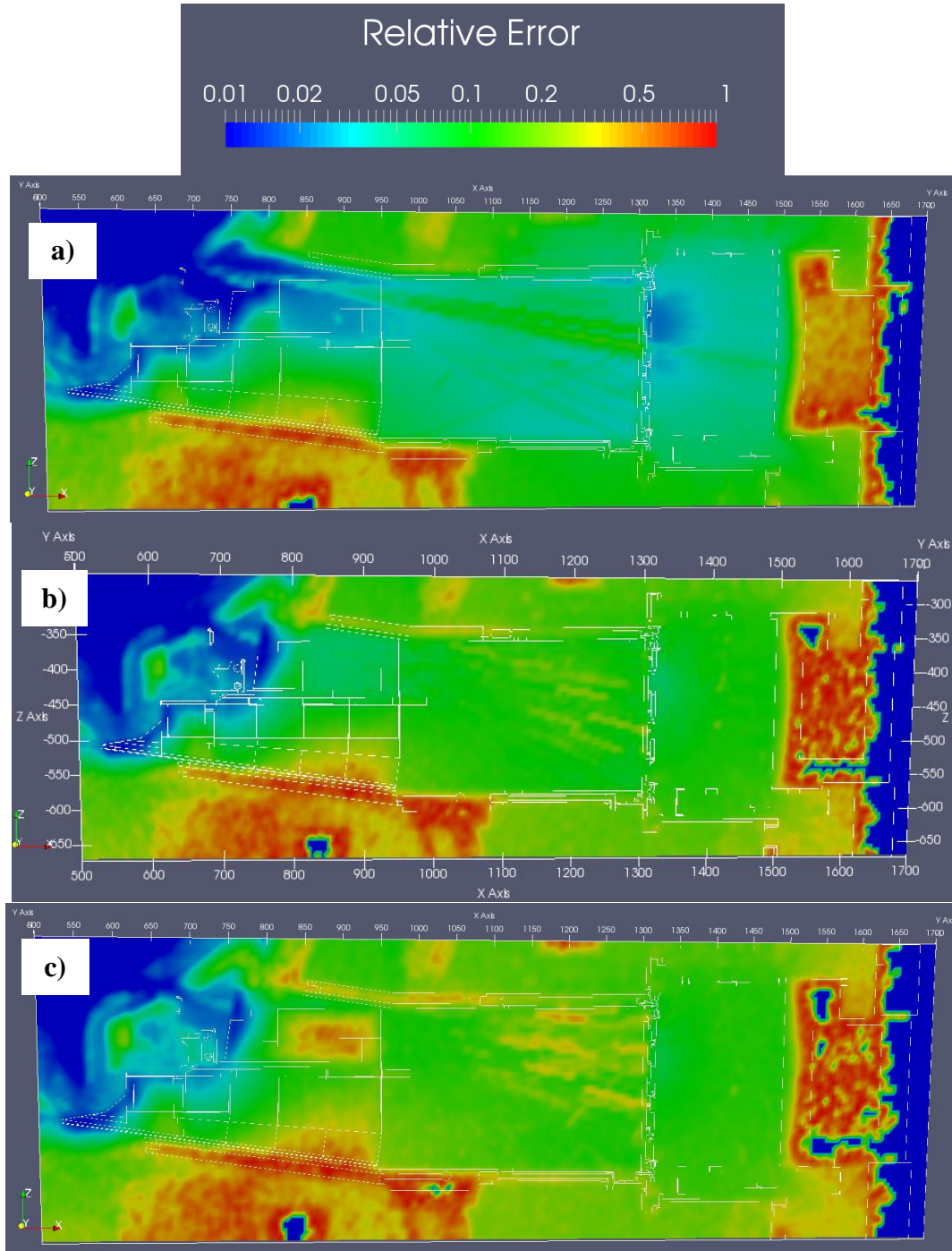


Figure 12.- Statistic relative error of the neutron fluence rate for the three cases evaluated; a) Case 1, b) Case 2, and c) Case 3

4. Conclusions

The MCNP baseline model of the RH-LP rack has been developed in this work, using the approved CAD model provided by ITER IO. This model has been inserted in the ITER MCNP model DGEPP 01102015 V1.1 04042016 EPY, which was modified to accommodate perfectly all the lower port components, like the support pads, the central cassette outer rail, the toroidal divertor rails, the pipes supports and the water cooling pipes.

Neutron transport calculations were performed to evaluate the radiation maps in ITER operation mode. The main conclusion supported by these calculations is that the neutron streaming is high considering the baseline components of the RH-LP rack. This baseline model is affected by an intense neutron streaming; in fact, a neutron fluence rate of $1 \cdot 10^{10}$ n/cm²s reaches the closure flange. According to that, a neutron shielding study has been successfully developed to reduce the neutron streaming, i.e. all the shielding blocks tested have worked properly. They have managed to reduce the neutron fluence rates along the lower port and IS area. With the shielding blocks tested in case 2, Figure 8, the neutron fluence rate in the closure flange decreases one order of magnitude from $1 \cdot 10^{10}$ to $1 \cdot 10^9$ n/cm²s. In addition, adding to the case 2 the large shielding block behind the upper shielding block in case 3, Figure 9, the zones with neutron fluence rate higher than $1 \cdot 10^9$ n/cm²s decreases significantly along the lower port, respect to the case 2.

Further engineering and integration studies will be necessary to assess if the implementation of additional shielding is feasible, like the shielding blocks proposed in this work, as this study has shown that such an examination would be worthwhile.

5. Acknowledgements

This work has been supported by ITER IO within the framework of the service contract N° 4200001696. This work was carried out using an adaptation of the C-lite MCNP model which was developed as a collaborative effort between the FDS team of ASIPP China, University of Wisconsin-Madison, ENEA FRASCATI, CCFE UK, JAEA NAKA, and the ITER ORGANIZATION. The views and opinions expressed herein do not necessarily reflect those of the ITER Organization.

6. References

- [1] M. Merola, F. Escourbiac, R. Raffray, P. Chappuis, T. Hirai, A. Martin, "Overview and status of ITER internal components Fusion Engineering and Design 89 (2014) 890–895
- [2] J. González, M. Clough, A. Martin, N. Woods, A. Suarez, G. Martinez, G. Stefan, Ma Yunxing, "Distribution of the In-Vessel Diagnostics in ITER Tokamak", Fusion Engineering and Design 114 (2017) 180–186.
- [3] O. Bede, J. Palmer, V. Udintsev, T. Zhao, IS-23-55-014 Diagnostic Rack remote handling (on the machine) ITER IO IDM UID PTKKZM 27 Jan 2015/1.1/Approved
- [4] SpaceClaim CAD software. 2016, Web-site: <http://www.spaceclaim.com>
- [5] F. Mota, R. Juarez, "D04 - Completion of design of MCNP Generic Diagnostic Rack", (2016) ITER D T9B5MM, private communication.
- [6] R. Juarez, "Neutronics guidelines for ITER Diagnostics Division, (2015)", ITER_D_RLVRDP, private communication.
- [7] Y. Wu, FDS Team, "CAD-based interface programs for fusion neutron transport simulation", Fusion Engineering and Design 84 (2009) 1987 – 1992
- [8] WU Y. et al. "CAD-based Monte Carlo program for integrated simulation of nuclear system superMC" Ann. Fusion Energy 82 (2015) 161–168
- [9] C-lite v2, personal communication, contact Michael.Loughlin@iter.org and Eduard.Polunovskiy@iter.org, private communication.
- [10] Aljaž Kolšek, Rafael Juarez, Antonio Lopez, Gabriel Pedroche, Arkady Serikov, Raul Pampin, Luciano Bertalot, Victor Udintsev, Julio Guirao, Javier Sanz, "Shutdown dose rate mitigation in the ITER upper ports", Fusion Engineering and Design, in press (2018), ISSN 0920-3796, <https://doi.org/10.1016/j.fusengdes.2018.01.070>.

-
- [11] V. Barabash, M. Loughlin, Chemical composition and impurity requirements for materials: Project Issue Management / PIM-169 (REYV5V v2.3) (2016) , private communication.
- [12] L. X5 Monte Carlo Team, "MCNP — A General Monte Carlo N-Particle Transport Code, version 5, 2008.
- [13] FENDL-2.1 Library Home: <http://www-nds.iaea.org/fendl21/>
- [14] MCNP – General Monte Carlo N-Particle Transport Code, versión 5, Manual VOL 1, april 24, 2003 (Revised 2/1/2008) LA-UR-03-1987